Small Animal Imaging in Oncology Drug Development

5

Joseph D. Kalen and James L. Tatum

5.1 Introduction

Major advances in small animal imaging have been made during the last two decades encompassing a full array of platforms that image along the electromagnetic spectrum from MRI (10^{0}–10^{1} m), optical (10^{-6} m), X-ray (10^{-9} m), to nuclear (10^{-11}–10^{-12} m). This in part has been facilitated by the National Cancer Institute (NCI), National Institutes of Health (NIH) through the support of Small Animal Imaging Research Programs (SAIRP), and other initiatives to increase the availability of small animal imaging platforms and develop the expertise in the use of these methods. While the primary application of these new techniques has been research tools to answer scientific questions especially related to the understanding of in vivo systems, another area of interest has been the introduction of imaging-based in vivo assay systems for drug development in oncology. In fact, a major effort has been undertaken to integrate in vivo imaging biomarker development with in vitro biomarker development in contrast to the historical scenario of applying imaging only late in the development plan, leading to the conundrum of validation of imaging while trying to employ imaging as a biomarker.

Drug development is a high-risk business in which late-stage failures are especially costly, with an average cost (capitalized and out of pocket) (2016) of

J. D. Kalen (✉)
Small Animal Imaging Program, Laboratory Animal Sciences Program, Frederick National Laboratory for Cancer Research Sponsored by the National Cancer Institute, Frederick, MD, USA
e-mail: kalenj@mail.nih.gov

J. L. Tatum
Cancer Imaging Program, Division of Cancer Treatment and Diagnosis, National Cancer Institute, NIH, Bethesda, MD, USA
e-mail: james.tatum@nih.gov

C. Kuntner-Hannes, Y. Haemisch (eds.), *Image Fusion in Preclinical Applications*, https://doi.org/10.1007/978-3-030-02973-9_5

approximately $3.95B ($1.528B (preclinical) and $2.43B (clinical)) normalized to 2013 dollars [1]. Trends in capitalized costs since the 1970s (based on 2013 dollars) have shown dramatic increases in preclinical and clinical costs, 1007% and 2085%, respectively [1]. Although the monetary costs are obvious, the opportunity cost of such failures, consuming valuable resources and time, may lead to more significant health cost. The focus on targeted agents has further complicated the development process. Unfortunately, late-phase failures with new targeted agents are not uncommon and frequently the result of inadequate biomarker development. It has been reported that robust biomarkers are essential to successful drug development and can improve the success rate for phase I to drug approval as much as 25.9% (with biomarkers) as compared to 8.4% (without biomarkers) [2]. In oncology, drugs and especially new pathway-specific drugs non-context in vitro assays may not be adequate when applied to clinical scenarios which are highly contextually based. Small animal imaging with image fusion encompassing different modalities and molecular probes has the potential to enhance our understanding of drug candidates and combinations in context by serving as an in vivo assay system allowing evaluation of various biomarkers in the complex biologic system of cancer. While imaging of small animals is now routinely performed daily in many labs, converting such imaging to an in vivo assay for drug development is significantly more challenging.

Performing small animal imaging in the context of an in vivo assay for drug development encompasses numerous aspects: standardization of equipment processes (SOPs) including quality control and quality assurance, data acquisition, analysis, and validation of output with respect to a gold standard (i.e., pathology) [3–6] are all important requirements for developing an assay for drug development. Furthermore, other aspects such as animal handling, anesthesia and understanding its effect on the animals physiology (pulmonary and cardiac functions and stress levels) [7–11], personnel safety for handling animals that contain toxic chemicals [12], validation of animal model platforms [5], multi-animal throughput to obtain statistical significance, and multi-imaging platforms to discern a drugs effect on the various physiological [13], anatomical, and molecular pathways are all significant aspects for developing a robust drug development in vivo assay. Numerous references have been cited that describe the above factors for performing small animal imaging.

The main aspect of this book is to provide an overview of multimodality preclinical imaging, and this chapter is intended to demonstrate how these techniques can be implemented for oncology drug development. Initial utilization of in vivo imaging incorporated clinical scanners for simple analysis of anatomical tumor volumes or a metabolic function using the clinically available radiopharmaceutical 2-deoxy-2-(^{18}F)fluoro-D-glucose [^{18}F]FDG. As equipment manufacturers developed and modified scanners explicitly for small animals, incorporating higher spatial image resolution and faster acquisitions to analyze the small animal's rapid heart, pulmonary, and biological rates, these scanners were providing in vivo techniques to allow researchers the ability to question and comprehend specific processes pertinent to developing an oncologic drug. Furthermore, due to the inherent physics of each system's attributes to acquire data along the electromagnetic spectrum and

Table 5.1 Comparison of preclinical in vivo imaging modalities

Modality	Image resolution (μm)	3D capability (tomography)	Probe sensitivity (mol/L)	Intrinsic contrast	Amount of probe required	Activatable probes	Dynamic studies
X-ray CT	5	Yes	N/A	Yes		No	No
MRI	170	Yes	10^{3} to 10^{-5}	Yes	μg–mg	No	Yes
PET	1000	Yes	10^{-11} to 10^{-12}	No	ng	No	Yes
SPECT (determined by collimator and head orientation)	150–2000	Yes	10^{-10} to 10^{-11}	No	ng	No	Yes
Ultrasound	30	Limited (small volume)	High (not well characterized)	Yes	μg–mg	Yes	Yes
Photo-acoustic	44–75	(Small volume)	10^{-7}				Yes
Bioluminescence	>1000	Limited (semi-quantitative)	10^{-15} to 10^{-17}	Yes	μg–mg	Yes (?)	Yes (2D)
2D fluorescence	>1000	No	10^{-9} to 10^{-12}	Yes	μg–mg	Yes	Yes
Fluorescence tomography	<1000	Semi-quantitative	10^{-9} to 10^{-12}	Yes	μg–mg	Yes	No

utilization of various molecular imaging agents to probe specific pathways (Table 5.1), it has become necessary to incorporate numerous modalities to investigate the micro- and macro-biologic system for drug development.

5.2 Development and Validation of Model Platforms

To understand a drugs interaction within a biologic system, pertinent animal models have been established, from the simple subcutaneous (sc) injection of human cells to orthotopic models to genetically modified mouse models (GEMMs) incorporating knock-in, knockout, and CRISPR [14–16] technologies. Development of mouse model platforms for oncology drug development must also be validated utilizing histotechnological processes with respect to pathological standards such as angiogenesis (thymidine) and apoptosis (caspases, FITC-labeled Annexin V) [17]. Research groups such as the Biological Testing Branch, Division of Cancer Treatment and Diagnosis, and the Center for Advanced Preclinical Research (CAPR), Center for Cancer Research, both within NCI, have developed and fully characterized various xenograft models incorporating both human cells and tumor fragments and GEMM models (pancreas, lung, and ovarian) for testing new drugs against standard clinical therapies [18, 19].

In addition to the primary tumor, model platforms for the study of metastasis should be included in the repertoire [20]. Metastasis of cancer cells from a primary tumor is a leading cause of death [21], and early detection for timely therapeutic

intervention with serial in vivo imaging would greatly improve clinical outcomes. Bioluminescence imaging (BLI) has been shown to be sensitive with the ability to image few cells, correlates to tumor volume as validated by gadolinium contrast MRI, and provides rapid imaging for high throughput [22]. Unfortunately, it only provides 2D images, and the depth penetration of light is limited to a few cm. On the other hand, utilizing BLI to first determine the presence of a metastatic signal (pre-screening technique), due to the BLI higher sensitivity and the higher throughput with respect to 3D small-bore modalities, BLI can improve utilization of higher-cost 3D modalities. This demonstrates that multimodality imaging does not mandate concurrent image acquisitions. Utilizing one modality to screen for presence of metastasis can greatly enhance utilization of another modality. Furthermore, due to the metastasis textural characteristics (i.e., echogenicity), a higher spatial resolution scanner (i.e., 30 μm for ultrasound) might not detect the metastatic lesion, whereas a lower spatial resolution scanner (i.e., 170 μm for MRI) can provide a higher-contrast signal (Fig. 5.1), such as in a T2* MRI sequence.

Further advancements in oncology animal models capturing the cell-autonomous (genetic and epi-genetic) and non-cell autonomous (stromal) aspects of tumor heterogeneity improve the understanding of patient-specific responses to therapy (precision medicine); thus cancer researchers have instituted patient-derived xenograft (PDX) animal model studies [23, 24]. The heterogeneity in the tumor fragment can be attributed to the tumor matrix that is transplanted with the tumor. This matrix tends to persist as the tumor grows, eventually becoming permeated and dissolving into the tumor. While there is mild heterogeneity seen in cellular base xenografts,

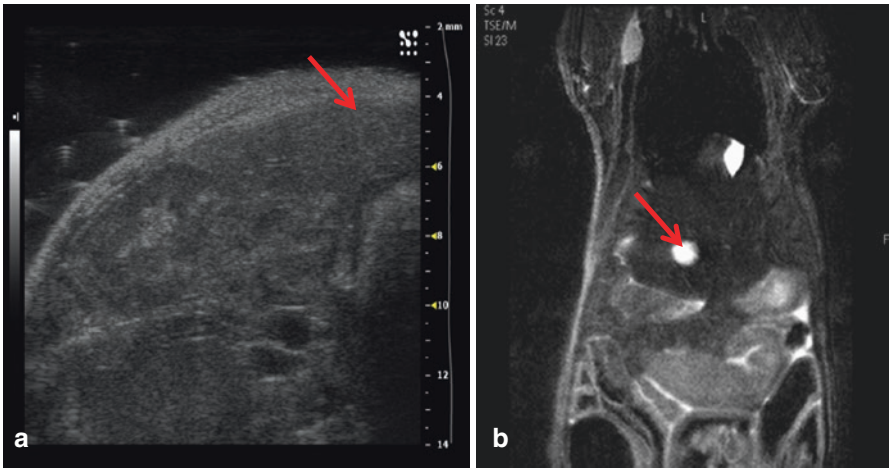

Fig. 5.1 These two images demonstrate the marked difference in image contrast (red arrow) for a metastatic lesion (**a**) isoechoic with capsule in a B-mode ultrasound scanner (30 μm image resolution) and (**b**) high-contrast T2 signal in a 3 T MRI (150 μm image resolution) image with coils specific for small animals. While the resolution of US is greater than MRI, it is more difficult to compare lesions longitudinally on US. However, small animal US provides greater capability for dynamic characterization of individual lesions

the heterogeneity in the fragment group is far more typical of what is seen throughout the tumor growth in this group and is hypothesized to be more representative of the native in vivo microenvironment.

5.3 In Vivo Imaging for Oncology Translational Research

Within the vast array of technologies for small animal imaging, there are many opportunities to design imaging-based experiments to answer complex biological questions. However, in drug/therapy development, the requirements become more demanding and less flexible, shifting from an imaging experiment to an in vivo assay. To institute an in vivo assay, three key elements must exist: (1) relevant biomarker matched to imaging capability, (2) highly reproducible results, and (3) efficient throughput. Another aspect of importance is the ability to translate nonclinical assays to clinical research as needed for future development.

As previously discussed, this requires rigorous SOPs, a validated animal model, imaging equipment quality control, close attention to animal handling, quality control of probes, contrast agents, and radiopharmaceuticals, close adherence to acquisition protocols and a standardized analysis. The routine incorporation of both positive and negative pathological standards is also critical.

This conversion of the imaging experiment to an in vivo assay requires the development of an imaging assay platform that incorporates the appropriate validated model and a highly controlled imaging protocol designed to optimally measure the biomarker of interest. For the assay to be practical, both logistical and physiologic barriers need to be minimized by incorporation of such practices as keeping intravenous administrations to a minimum, reducing anesthesia sessions, and using systems that allow concurrent imaging of animals but allowing constant monitoring.

The implementation of small animal imaging in oncology drug development will now be described using three case study examples.

5.3.1 Case Studies

5.3.1.1 Development of an Imaging Platform Consisting of an Animal Model and MR Technique

Colorectal cancer (CRC) is the third most common cancer in the United States, and the American Cancer Society estimated that in 2018 there will be 97,220 new cases and 50,630 deaths [25] and that chronic inflammation, such as ulcerative colitis and Crohn's disease, is associated with increased risk of CRC. To study colorectal cancer, animal models as an imaging assay platform can assist in the assessment of the initial stages of cancer and therapy response.

Conventional micro-endoscopes can provide appropriate information on colorectal cancer, i.e., imaging polyps, but risk perforating the colon or obstruction of the image due to bleeding associated with colitis. 3D in vivo imaging (i.e., virtual colonoscopy) can image the early phases of cancer, and utilizing various imaging agents

can probe molecular pathways for characterization, including when altered by a drug. Clinically, X-ray CT has been a standard in performing virtual colonoscopy due to its rapid image acquisition. Preclinical X-ray CT scanners can provide information on polyp growth [26, 27] but are unable to provide the high tissue contrast necessary to discern normal and inflamed lumen tissue from surrounding tissue without resulting in high-radiation doses, especially in preclinical studies when serial imaging is required. Another method used in the clinic, magnetic resonance colonography (MRC), can discern normal and inflammatory tissue utilizing the dark lumen technique with either water or gas to expand the colon followed by IV contrast (Gd-chelate)-enhanced T1w MRI sequence, where water, if used as an enema, remains dark. T2w MRI is required to discern inflammatory tissue and also provides a rapid acquisition for high-throughput; unfortunately the water enema results in a bright signal. Preclinical MRI colorectal studies have utilized other techniques such as fecal tagging [28], and water enema [29], which unfortunately creates a bright lumen in T2w images making it difficult to distinguish normal from inflamed colonic mucosa, especially for researching drugs for chronic inflammation (pre-CRC).

Thus, the aim was to develop an imaging platform consisting of a mouse model and an adjusted MR protocol to study colorectal cancer. The in vivo MRI protocol should provide several important components: noninvasive serial imaging to monitor tumor progression and tissue inflammation, artifact-free imaging on T1w and T2w MRI sequences, enhanced image contrast (high signal-to-noise ratio: SNR) to discern inflamed and normal lumen tissue from surrounding tissue, quantitative imaging, and high throughput.

FVB/N mice were dosed (10 mg/kg, IP route) with a chemical carcinogen azoxymethane (AOM) and exposed 1 week later to the colonic irritant dextran sodium (DSS) [1–5% DSS dissolved in drinking water] for five cycles (5 days DSS and 16 days normal water) to develop the inflammation-induced colorectal cancer mouse model [30]. The virtual MRI colonoscopy technique implemented an enema procedure [31] using 1 mL of Fluorinert FC-770 (perfluorotri-n-butylamine, molecular formula of $C_{12}F_{27}N$), which does not create a MRI signal due to the lack of hydrogen atoms, and has been used in MRI imaging of human prostate cancer. Prior to MRI imaging, the enema was administered with a 20-G gavage syringe containing 0.6 mL of Fluorinert. The enema tubing was connected to a syringe pump and maintained at a continuous rate of 25 μL/min to maintain the colon distended during the imaging procedure. MRI (T1w and T2w) images were acquired pre- and post-contrast (gadopentetate dimeglumine (Gd-DTPA), 0.2 mmol/kg, IV injection, 150 μL/min infusion). Figures 5.2 and 5.3 demonstrate the utilization of a Fluorinert enema with MRI for virtual colonoscopy in the development of an animal model assay platform for the study of inflamed CRC. This standardized technique, incorporating both modality and animal model, provides for an assay platform for the study of drug efficacy studies for chronic inflammation (pre-CRC). In addition, the ability to fuse images from other modalities to virtual MRC can further enhance the information on molecular pathways in drug efficacy studies.

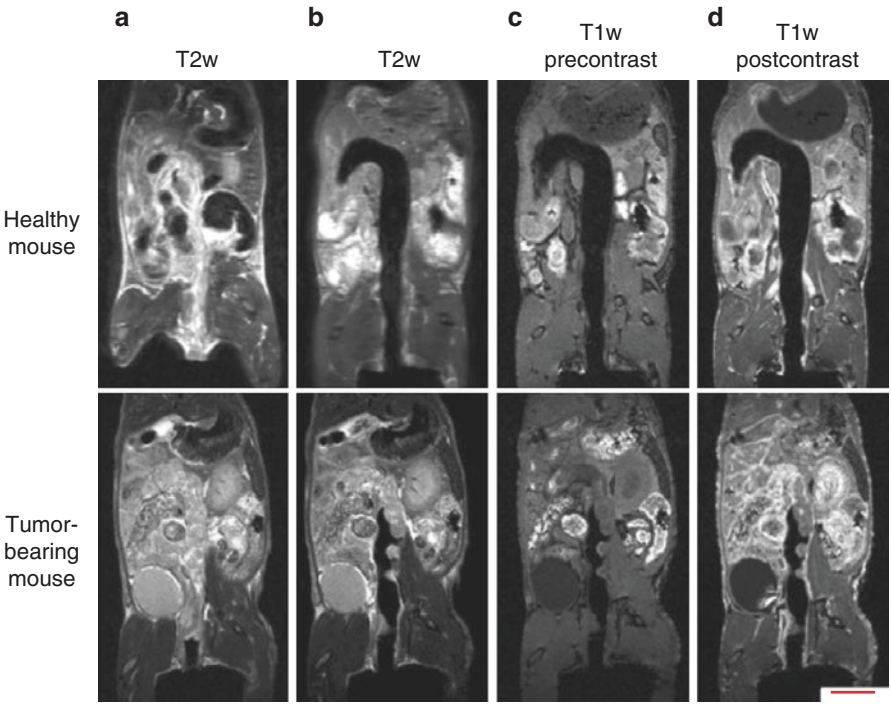

Fig. 5.2 3.0 T MR images of the mouse colon of healthy (top) and tumor-bearing mice (bottom row). (**a**) Coronal T2w image before Fluorinert enema infusion. (**b–d**) After Fluorinert enema: T2w image (**b**); T1w pre-contrast (**c**); and T1w post-contrast (Gd-DTPA) image (**d**). Scale bar, 5 mm. Ileva L et al. Nature Protocols, (2014), 9(11), 178–2682–2692. DOI:https://doi.org/10.1038/nprot.2014.178

5.3.1.2 Probe Validation: Nuclear Versus Optical Imaging

One major aspect for the development of an oncology drug as an in vivo assay is the development of a relevant biomarker matched to an imaging capability. One such drug, panitumumab (Vectibix), an anti-HER1 mAb, is a fully human mAb with minimal immunogenicity when injected intravenously. It is FDA approved for the treatment of HER1-expressing colorectal cancers, and is being evaluated in patients with other types of HER1-expressing cancers, such as breast, lung, head and neck, renal, and ovarian tumors [32]. The epidermal growth factor receptor (EGFR, erb1, HER1) is a glycoprotein belonging to subclass I of the tyrosine kinase receptor super family [33], disregulated in a variety of cancers [34], and is associated with disease progression and treatment resistance. Panitumumab binds to the domain III of HER1 and is rapidly internalized, leading to downregulation of cell surface HER1. It also arrests the cell cycle and inhibits tumor growth by suppressing the production of proangiogenic factors (VEGF, IL-8) by tumor cells [35].

To investigate a labeled panitumumab to risk-stratify clinical patients or as an intraoperative diagnostic probe for image-guided surgery, various subcutaneous

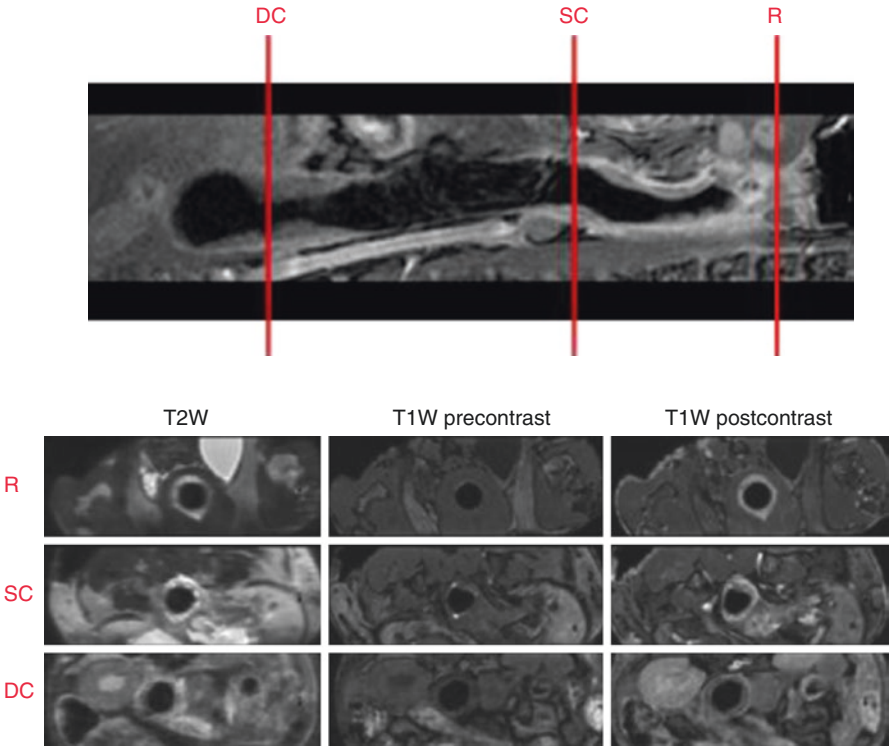

Fig. 5.3 The MRI sagittal colon plane (top) provides the relative positions in the transverse plane for the rectum (R), sigmoid colon (SC) and descending colon (DC). The relative planes in the transverse slices (bottom) are generated from the T1w and T2w coronal 3D images demonstrating the Fluorinert enema and the enhancement of the lumen for studying inflammation in pre-CRC drug studies. Ileva L et al. Nature Protocols, (2014), 9(11), 178–2682–2692. DOI:https://doi.org/10.1038/nprot.2014.178

athymic nude female breast cancer xenograft tumor cell models have been developed with respect to HER1 expression (MDA-MB-469; high HER1, MDA-MB-231; mid HER1, and BT-474; low HER1). Panitumumab can be dual-labeled with a fluorescence dye (i.e., IRDye 800, optical component) and a radionuclide (i.e., 111-indium, SPECT component and/or 89-zirconium, PET component) for testing the various scenarios and models to visualize and quantify panitumumab uptake into the tumor and organs. Dual labeling is more time-consuming and costly compared to single labeling, with the caveat that quantified results of a single-labeled drug can be compared (molecular probe uptake into the tumor and organs) between modalities while utilizing standard animal handling techniques. Furthermore, dual labeling of radionuclides (i.e., SPECT and PET) might not be feasible due to the higher-energy PET photons (511 keV) penetration of the lower photon energy SPECT collimators. Figure 5.4 demonstrates dual-modality PET/CT coronal slices for the biodistribution of [^{89}Zr] panitumumab in various tumor-bearing animal

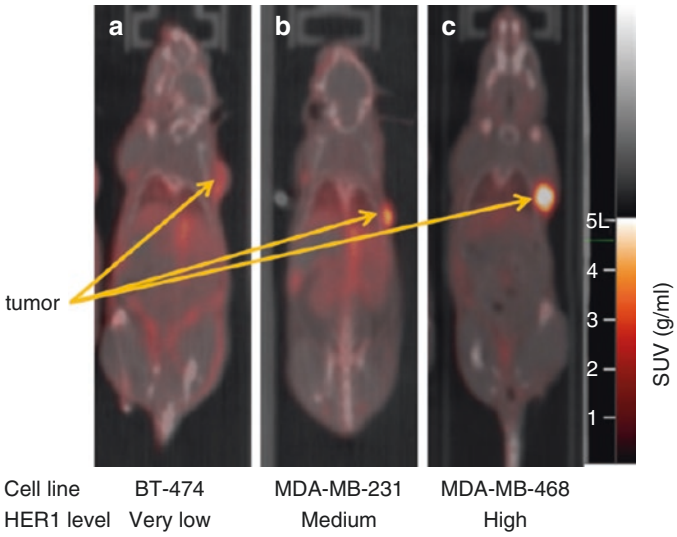

Fig. 5.4 Coronal slices demonstrating tumor uptake of ^{89}Zr-panitumumab in various subcutaneous athymic nude female xenograft models; 10.18 ± 1.24 MBq of ^{89}Zr-panitumumab were administered intravenously via tail vein, and a 5-min CT scan followed by a 30-min static PET scan was performed at 96 h postinjection. The probe uptake into the tumor correlates with the HER1 protein expression. Orange arrows point to the representative HER1 tumors. Sibaprasad Bhattacharyya et al. Zirconium-89 labeled panitumumab: a potential immuno-PET probe for HER1-expressing carcinomas. Nuclear Medicine and Biology, 2013, 40, 451–457, https://doi.org/10.1016/j.nucmedbio.2013.01.007

models and correlation to the HER1 protein expression [36]. The same HER1 expression animal model(s) were later implemented in an epi-fluorescence imaging study for the determination of [IRDye 800]-labeled panitumumab for an intraoperative diagnostic probe for image-guided surgery [37]. Figure 5.5 demonstrates epi-fluorescence imaging for the HER1 animal models, resulting in similar probe uptake into the tumor(s) with respect to the HER1 expression, and Fig. 5.6 exhibits the correlation of the panitumumab imaging probe ([^{89}Zr] and [IRDye 800]) uptake between the different modalities. This case study demonstrates that providing a modulated signal (i.e., HER1) will enable the quantitative investigation of the underlining biomarker and that quantitation of the molecular biomarker with respect to the modality (i.e., fluorescence or nuclear probe) provides for an accurate technique for comparison between modalities without the necessity of costly dual labeling.

5.3.1.3 Multimodality Probe Development

Inhalation of asbestos fibers is the primary cause of malignant pleural mesothelium (MPM), a highly lethal cancer affecting the lung pleural, and has been shown to result in increased tissue HER1 expression [38]. X-ray CT and MRI have difficulties distinguishing nonmalignant features of scarring and fibrosis from tumor tissue;

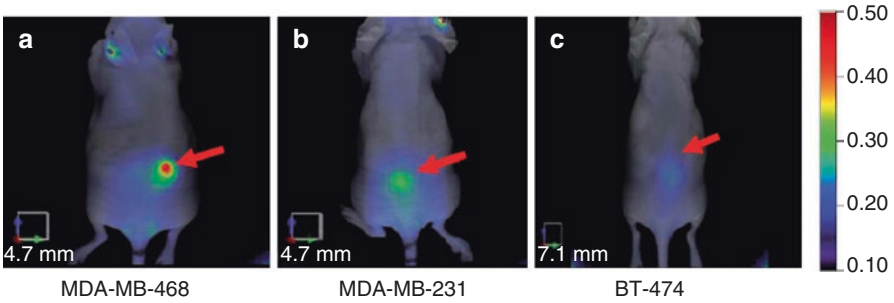

Fig. 5.5 2D epi-fluorescence images of panitumumab–IRDye800 of various HER1-expressing tumor (MDA-MB-468, MDA-MB-231, BT474) bearing athymic nude female mouse models at 24 h postinjection (100 mL of 1 mg mL^{-1} conjugate). Red arrows point to the representative HER1 tumors. The probe uptake into the tumor correlates with the HER1 protein expression. Trace amounts of tracer accumulated in ears probably due to the inflammation caused by ear punch. Sibaprasad Bhattacharyya et al. Synthesis and biological evaluation of panitumumab–IRDye800 conjugate as a fluorescence imaging probe for EGFR-expressing cancers. Med. Chem. Commum., 2014, DOI: https://doi.org/10.1039/c4md00116h

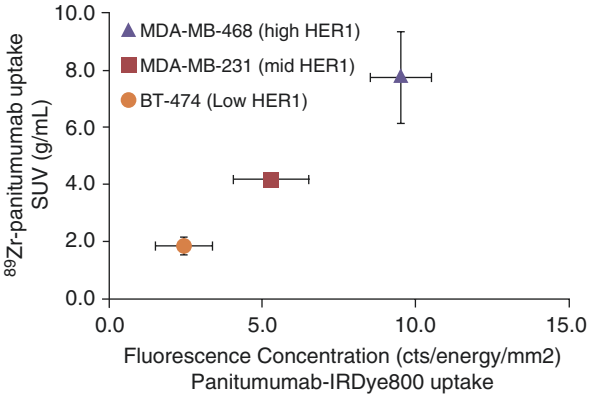

Fig. 5.6 Uptake of panitumumab labeled with IRDye800 or [^{89}Zr] in different tumor xenografts with high, medium, and low EGFR expression, as measured by radioactive counts or fluorescence, is highly correlated. Sibaprasad Bhattacharyya et al. Synthesis and biological evaluation of panitumumab–IRDye800 conjugate as a fluorescence imaging probe for EGFR-expressing cancers. Med. Chem. Commum., 2014, DOI: https://doi.org/10.1039/c4md00116h

while the high specificity of [^{18}F]FDG PET for tumor imaging is successful, unfortunately high FDG uptake is also observed in benign inflammatory processes. Unfortunately, the X-ray CT used in most preclinical scanners is designed for PET photon attenuation correction and/or anatomical-functional image fusion that does not provide for the ability to segment the various tissues (organs). Therefore, localization of the molecular probe in the tumor is poorly differentiated from the surrounding tissues, which can result in significant quantitative issues depending on the preclinical animal model. Nyak et al. [39] studied MPM in an orthotopic (NCI-H226 and MSTO-211H mesothelium cells) MPM mouse model, fusing

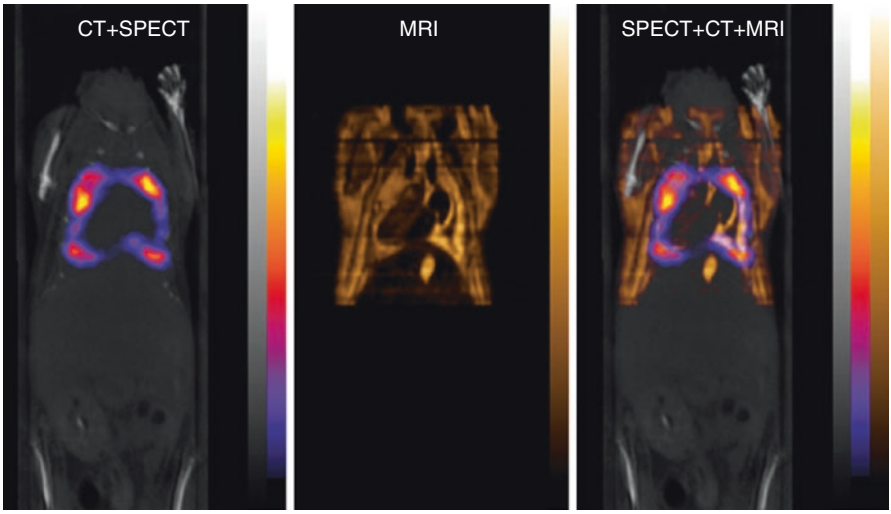

Fig. 5.7 Representative coronal sections in female athymic (NCr) nu/nu mouse bearing orthotopic NCI-H226 cells injected intravenously via tail vein with 2.0 MBq of ^{111}In-CHX-A"-DTPA–panitumumab. Images were acquired 5 days after the injection of radiolabeled panitumumab. Radiology 267, 2013: 173–182. DOI: https://doi.org/10.1148/radiol.12121021

panitumumab labeled with [^{111}In] for SPECT/CT with anatomic images from a 3.0 T MRI, exhibited in Fig. 5.7, demonstrating the enhancement of a multimodality study for both diagnostic and prognostic tools for the enhancement in the classification and assessment of the patients' disease state.

5.3.1.4 Case Studies Summary

The first examples (colorectal cancer and panitumumab) demonstrate the validation strategy that coupling an imaging probe or technique with an imaging platform(s) has the characteristics of an assay. Specifically, in the panitumumab case, providing a modulated signal over the relevant biological scale will enable the quantitative investigation of the underlining biomarker, which in this case is HER1. The last case (multimodality probe development) demonstrates the enhancement of multimodalities to improve tissue characterization by reducing the false-positive features of a single modality. This case study further exemplifies in a multimodality study that establishing SOPs for equipment QC, animal handling, anesthesia, and image quantitation that utilizes animal models that are validated with respect to pathological standards is essential for the development of in vivo imaging assays.

5.3.1.5 Future

Multimodality preclinical imaging will be a requirement in oncology drug development to understand the effect of treatment(s) on the various molecular pathways transforming the tumor microenvironment. The incorporation of patient-derived xenografts (PDX) into preclinical and co-clinical studies will correspondingly require multimodalities due to the multi-scale in tumor heterogeneity.

To understand and analyze these spatially distinct regions within a tumor as probed by multimodalities, investigators are incorporating texture analysis (fractals and lacunarity) [40–42]. For example, Dominietto et al. evaluated pattern analysis in a murine efficacy study investigating tumor angiogenesis [43]. MRI studies evaluated tumor blood volume and permeability at baseline and post-therapy. The authors evaluated the MRI images utilizing both standard histogram analyses (average values within a region of interest (ROI)) and pattern analysis (shape and texture) and concluded that the standard histogram was insensitive to determine therapeutic response, while pattern analysis appeared to be sensitive to tumor textural changes due to treatment. In addition to evaluating texture analysis in different modalities for clinical and preclinical studies, other authors are evaluating the effect of reconstruction algorithms on textural analysis, such as in PET imaging due to the limited number of projections and higher noise component [44, 45].

To improve the integration of multimodalities, especially for co-clinical endeavors, the National Cancer Informatics Program, which includes several NIH/National Cancer Institute Divisions (Center for Biomedical Informatics and Information Technology (CBIIT)), Cancer Imaging Program/Division of Cancer Treatment and Diagnosis), and several academic and industry partners, implemented a working group and developed a standard radiological image header (DICOM) for small animal imaging (Work Group 30: http://dicom.nema.org/dicom/geninfo/Strategy.pdf). These standards provide a framework for quantitative comparison of multimodality preclinical and clinical image sets utilizing identical image analysis algorithms. These headers will also allow for the incorporation and fusion of ex vivo pathological slides and molecular analysis, to include the full spectrum and multi-scale aspects for understanding the tumor microenvironment.

The future of multimodality imaging in small animals will provide an important basis for in vivo assay development in oncology drug discovery, improving quantitative measurement of therapeutic response, understanding the tumor microenvironment, and the integration of emerging fields such as radiomics and radiogenomics for improved patient outcomes.

Acknowledgments This project has been funded in whole or in part with federal funds from the National Cancer Institute, National Institutes of Health, under Contract No. HHSN261200800001E. The content of this publication does not necessarily reflect the views or policies of the Department of Health and Human Services, nor does mention of trade names, commercial products, or organizations imply endorsement by the U.S. Government Modified per federal agency (NIH).

Frederick National Laboratory for Cancer Research is accredited by AAALAC International and follows the Public Health Service Policy for the Care and Use of Laboratory Animals. Animal care was provided in accordance with the procedures outlined in the "Guide for Care and Use of Laboratory Animals" (National Research Council, 2011; National Academies Press, Washington, D.C.).

References

1. DiMasi JA, Grabowski HG, Hansen RW. Innovation in the pharmaceutical industry: new estimates of R&D costs. J Health Econ. 2016;47:20–33. https://doi.org/10.1016/j.jhealeco.2016.01.012.

2. Thomas DW, Burns J, Audette J, Carroll A, et al. Clinical development success rates 2006–2015, BioIndustry analysis. http://www.amplion.com/clinical-development-success-rates?hsCtaTracking=7e38cfe3-248d-440b-a7e4-c038acfa6eb2%7Ca6180579-5624-4deb-ac76-35b512407bd1
3. Vanhove C, Bankstahl JP, Krämer SD, Visser E, Belcari N, Vandenberghe S. Accurate molecular imaging of small animals taking into account animal models, handling, anesthesia, quality control and imaging system performance. EJNMMI Phys. 2015;2:31. https://doi.org/10.1186/s40658-015-0135-y.
4. Kinahan P, Fletcher JW. PET/CT standardized uptake values (SUVs) in clinical practice and assessing response to therapy. Semin Ultrasound CT MR. 2010;31(6):496–505. https://doi.org/10.1053/j.sult.2010.10.001.
5. Sha W, Ye H, Iwamoto KS, Wong K-P, Wilks MQ, Stout D, McBride W, Huang S-C. Factors affecting tumor ^{18}F-FDG uptake in longitudinal mouse PET studies. EJNMMI Res. 2013;3:51. https://doi.org/10.1186/2191-219X-3-51.
6. Adiseshaiah PP, Patel NL, Ileva LV, Kalen JD, Haines DC, McNeil SE. Longitudinal imaging of cancer cell metastasis in two preclinical models: a correlation of noninvasive imaging to histopathology. Int J Molecul Imaging. 2014;2014:102702. https://doi.org/10.1155/2014/102702.
7. Fuchs K, Kukuk D, Mahling M, Quintanilla-Martinez L, Reischl G, Reutershan J, Lang F, Rocken M, Pichler BJ, Kneilling M. Impact of anesthetics on 3′-[^{18}F]fluoro-3′-deoxythymidine ([^{18}F]FLT) uptake in animal models of cancer and inflammation. Mol Imaging. 2013:1–11. https://doi.org/10.2310/7290.2012.00042.
8. Maier FC, Kneilling M, Reischl G, Cay F, Bukala D, Schmid A, Judenhofer MS, Röcken M, Machulla H-J, Pichler BJ. Significant impact of different oxygen breathing conditions on non-invasive in vivo tumor-hypoxia imaging using [^{18}F]-fluoro-azomycinarabino- furanoside ([^{18}F]FAZA). Radiat Oncol. 2011;6:165. https://doi.org/10.1186/1748-717X-6-165.
9. Fueger BJ, Czernin J, Hildebrandt I, Tran C, Halpern BS, Stout D, Phelps ME, Weber WA. Impact of animal handling on the results of ^{18}F-FDG PET studies in mice. J Nucl Med. 2006;47(6):999–1006.
10. Fuchs K, Kukuk D, Reischl G, Foller M, Eichner M, Reutershan J, Lang F, Rocken M, Pichler BJ, Kneilling M. Oxygen breathing affects 3′-deoxy-3'-^{18}F-fluorothymidine uptake in mouse models of arthritis and cancer. J Nucl Med. 2012;53:823–30. https://doi.org/10.2967/jnumed.111.101808.
11. Hildebrandt IJ, Helen S, Weber WA. Anesthesia and other considerations for in vivo imaging of small animals. ILAR. 2008;49(1):17–26. https://doi.org/10.1093/ilar.49.1.17.
12. Ileva LV, Bernardo M, Patel NL, Riffle LA, Graff-Cherry C, Robinson C, Difilippantonio S, Kalen JD. Challenges in performing preclinical imaging in a large cohort therapeutic efficacy study of murine cancer models. 64th AALAS National Meeting, Baltimore, MD, October 29, 2013.
13. Honndorf VS, Schmidt H, Wehrl HF, Wiehr S, Ehrlichmann W, Quintanilla-Martinez L, Barjat H, Ricketts S-A, Pichler BJ. Quantitative correlation at the molecular level of tumor response to docetaxel by multimodal diffusion-weighted magnetic resonance imaging and [^{18}F]FDG/[^{18}F]FLT positron emission tomography. Mol Imaging. 2014;(1) https://doi.org/10.2310/7290.2014.00045.
14. Yang H, Wang H, Shivalila CS, Cheng AW, Shi L, Jaenisch R. One-step generation of mice carrying reporter and conditional alleles by CRISPR/cas-mediated genome engineering. Cell. 2013;154(6):1370–9. https://doi.org/10.1016/2013.08.022.
15. The Jackson Laboratory, Bar Harbor, ME USA, https://www.jax.org/.
16. Tentler JJ, Tan AC, Weekes CD, Jimeno A, Leong S, Pitts TM, Arcaroli JJ, Messersmith WA, Gail Eckhardt S. Patient-derived tumor xenografts as models for oncology drug development. Nat Rev Clin Oncol. 2012;9:338–50. https://doi.org/10.1038/nrclinonc.2012.61.
17. Elmore S. Apoptosis: a review of programmed cell death. Toxicol Pathol. 2007;35(4):495–516.
18. Biological Testing Branch, Division of Cancer Diagnostics and Treatment, NCI, NIH: https://dtp.cancer.gov/organization/btb/default.htm
19. Center for Advanced Preclinical Research, Center for Cancer Research, NCI, NIH: https://ccr.cancer.gov/capr

20. van Marion DMS, et al. Studying cancer metastasis: Existing models, challenges and future perspectives. Crit Rev Oncol Hematol. 2015;97:107–17. https://doi.org/10.1016/j.critrevonc.2015.08.00.
21. Chaffer CL, Weinberg RA. A perspective on cancer cell metastasis. Science. 2011;331(6024):1559–64. https://doi.org/10.1126/science.1203543.
22. Troy T, Jekic-McMullen D, Sambucetti L, Rice B. Quantitative comparison of the sensitivity of detection of fluorescent and bioluminescence reporters in animal models. Mol Imaging. 2004;3(1):9–23.
23. Siolas D, Honnon GJ. Patient-derived tumor xenografts: transforming clinical samples into mouse models. Cancer Res. 2013;73(17):5315–9. https://doi.org/10.1158/0008-5472.CAN-13-1069.
24. Cassidy JW, Caldas C, Bruna A. Maintaining tumor heterogeneity in patient-derived tumor xenografts. Cancer Res. 2015;75(15):2963–8. https://doi.org/10.1158/0008-5472.CAN-15-0727.
25. American Cancer Society. Colorectal cancer. 2018.
26. Durkee BY, Weichert JP, Halberg RB. Small animal micro-CT colonography. Methods. 2010;50:36–41. https://doi.org/10.1016/j.ymeth.2009.07.008.
27. Boll H, Bag S, Nölte IS, Wilhelm T, Kramer M, Groden C, Böcker U, Brockmann MA. Double-contrast micro-CT colonoscopy in live mice. Int J Color Dis. 2011;26:721–7. https://doi.org/10.1007/s00384-011-1181-0.
28. Larsson AE, et al. Magnetic resonance imaging of experimental mouse colitis and association with inflammatory activity. Inflamm Bowel Dis. 2006;12:478–85.
29. Herborn CU, et al. Dark lumen magnetic resonance colonography in a rodent polyp model: initial experience and demonstration of feasibility. Investig Radiol. 2004;39:723–7.
30. Ileva LV, Bernardo M, Young MR, Riffle LA, Tatum JL, Kalen JD, Choyke PL. In vivo MRI virtual colonography in a mouse model of colon cancer. Nat Protoc. 2014;9(11):2682–92. https://doi.org/10.1038/nprot.2014.178.
31. Young MR, Ileva LV, Bernardo M, Riffle LA, Jones YL, Kim YS, Colburn NH, Choyke PL. Monitoring of tumor promotion and progression in a mouse model of inflammation-induced colon cancer with magnetic resonance colonography. Neoplasia. 2009;11(3):237–46. https://doi.org/10.1593/neo.81326.
32. Wu M, Rivkin A, Pham T. Panitumumab: human monoclonal antibody against the epidermal growth factor receptors for the treatment of metastatic colorectal cancer. Clin Ther. 2008;30:14–30. https://doi.org/10.1016/j.clinthera.2008.01.014.
33. Burgess AW. EGFR family: structure physiology signaling and therapeutic targets. Growth Factors. 2008;26:263–74. https://doi.org/10.1080/0897719080231284.
34. Ciardiello F, Tortora G. Anti-epidermal growth factor receptor drugs in cancer therapy. Expert Opin Investig Drugs. 2002;11:755–68. https://doi.org/10.1517/13543784.11.6.755.
35. Yang XD, Xia XC, Corvalan JR, Wang P, Davis CG. Development of ABX-EGF, a fully human anti-EGF receptor monoclonal antibody, for cancer therapy. Crit Rev Oncol Hematol. 2001;38:17–23. https://doi.org/10.1016/S1040-8428(00)00134-7.
36. Bhattacharyya S, Kurdziel K, Wei L, Riffle L, Kaur G, Hill GC, Jacobs PM, Tatum JL, Dorosho JH, Kalen JD. Zirconium-89 labeled panitumumab: a potential immuno-PET probe for HER1-expressing carcinomas. Nucl Med Biol. 2013;40:451–7. https://doi.org/10.1016/j.nucmedbio.2013.01.007.
37. Bhattacharyya S, Patel NL, Wei L, Riffle LA, Kalen JD, Hill GC, Jacobs PM, Zinn KR, Rosenthal E. Synthesis and biological evaluation of panitumumab–IRDye800 conjugate as a fluorescence imaging probe for EGFR-expressing cancers. Med Chem Commum. 2014; https://doi.org/10.1039/c4md00116h.
38. Faux SP, Houghton CE, Hubbard A, Pat- rick G. Increased expression of epidermal growth factor receptor in rat pleural mesothelial cells correlates with carcinogenicity of mineral fibres. Carcinogenesis. 2000;21(12):2275–80. https://doi.org/10.1093/carcin/21.12.2275.
39. Nayak TK, Bernardo M, Milenic DE, Choyke PL, Brechbiel MW. Orthotopic Pleural Mesothelioma in Mice: SPECT/CT and MRI Imaging with HER1-and HER2-targeted

Radiolabeled Antibodies. Radiology. 2013;267:173–82. https://doi.org/10.1148/radiol.12121021.
40. Asselin M-C, O'Connor JPB, Boellaard R, Thacker NA, Jackson A. Quantifying heterogeneity in human tumours using MRI and PET. Eur J Cancer. 2012;48:447–55. https://doi.org/10.1016/j.ejca.2011.12.025.
41. Soares F, Janela F, Pereira M, Seabra J, Freire MM. 3D lacunarity in multifractal analysis of breast tumor lesions in dynamic contrast-enhanced magnetic resonance imaging. IEEE Trans Image Process. 2013;22(11):4422–35. https://doi.org/10.1109/TIP.2013.2273669.
42. Goh V, Sanghera B, Wellsted DM, Sundin J, Halligan S. Assessment of the spatial pattern of colorectal tumor perfusion estimated at perfusion CT using two-dimensional fractal analysis. Eur Radiol. 2009;19:1358–65. https://doi.org/10.1007/s00330-009-1304-y.
43. Dominietto M, Lehmann S, Keist R, Rudin M. Pattern analysis accounts for heterogeneity observed in MRI studies of tumor angiogenesis. Magn Reson Med. 2013;70:1481–90. https://doi.org/10.1002/mrm.24590.
44. Leijenaar RTH, Nalbantov G, Carvalho S, van Elmpt WJC, Troost EGC, Boellaard R, Aerts HJWL, Gillies RJ, Lambin P. The efect of SUV discretization in quantitative FDG-PET Radiomics: the need for standardized methodology in tumor texture analysis. Sci Rep. 2015;5:11075. https://doi.org/10.1038/srep11075.
45. Buvat I, Orlhac F, Soussan M. J Nucl Med. 2015;56(11):1642–4. https://doi.org/10.2967/jnumed.115.163469.